PAPER Special Issue on Microwave and Millimeter-Wave Technology

Radiation Properties of Ring-Shaped Microstrip Antenna Array

Motohiko KOBAYASHI†, **Eko Tjipto RAHARDJO**†, **Shin-ichiro TSUDA**††, *Nonmembers* *and* **Misao HANEISHI**†, *Member*

SUMMARY In this paper, mutual coupling $|S_{21}|$ between R-MSA (ring-shaped microstrip antenna) elements was estimated by the EMF method based on the cavity model. Then, the validity of the proposed method was tested by experiments. The experiments confirmed satisfactory agreement between the computed and experimental data for $|S_{21}|$ in both E- and H-plane arrangements. In addition, a circularly polarized planar array composed of R-MSA elements was designed on the basis of the data of $|S_{21}|$. The experimental results of such a planar array demonstrated high performance in radiation pattern as well as axial ratio property. Furthermore, the active reflection coefficient $|\Gamma|$ in the R-MSA array was also investigated in both equilateral and square arrangements. The computed results of active reflection coefficient in the array demonstrated high performance in both arrangements.

key words: *R-MSA, mutual coupling, active reflection coefficient, planar array, microstrip antenna*

1. Introduction

A ring-shaped microstrip antenna (R-MSA) has been extensively studied by many researchers for more than a decade; this is because of its various advantages, namely, it permits reduction of antenna size and insertion of an MMIC-circuit module into the inner aperture of an R-MSA element, and easily allows excitation of circular polarization [1]–[4]. However, none of them have paid attention to mutual coupling effect $|S_{21}|$ and active reflection coefficient $|\Gamma|$ in an R-MSA array. As well known, in the designing of an array antenna, it is important to estimate mutual coupling $|S_{21}|$ as well as active reflection coefficient $|\Gamma|$. For this reason, we investigated both mutual coupling and active reflection coefficient for R-MSA planar arrays.

In this paper, first, the expression for mutual coupling between R-MSA elements is derived by means of the EMF method based upon the cavity model. This method has been used for the analysis of the mutual coupling of a usual circular (holeless) MSA array and is well known for its simplicity without sacrificing its versatility [5]. Moreover, some experimental studies on the mutual coupling of a two-element R-MSA array are carried out to test the validity of the computational results. The computed data of $|S_{21}|$ were found to well agree with the experimental ones. Furthermore, a circularly polarized (CP) planar array composed of CP R-MSA elements was fabricated using the data of $|S_{21}|$ obtained, and was tested at the C-band. The experimental results of such a planar array demonstrated high performance in radiation pattern as well as axial ratio property. Finally, active reflection coefficient $|\Gamma|$ in R-MSA arrays is calculated employing the cavity model. High performance in both equilateral and square arrangements was confirmed from the computed data of active reflection coefficient.

Manuscript received February 1, 1995.
Manuscript revised March 27, 1995.

†The authors are with the Department of Electrical and Electronic, Saitama University, Urawa-shi, 338 Japan.
††The author is with Personal Telecom Division, Sony Electronic Inc. (SEL), 5205 Fiore Terrace B205, San Diego, CA92122, USA.

2. Analytical Method

2.1 Analysis of Mutual Coupling in R-MSA Array

The basic configuration of an isolated R-MSA element is illustrated in Fig. 1. In this figure, the ring ratio (β) of patch antenna is denoted as $\beta = b/a$, where a and b are the radii of the outer and inner rings, respectively. Additionally, the R-MSA element used in this analysis is fed by a coaxial probe at distance ρ from the center of R-MSA. Considering the field distribution of the TM_{mn0} mode excited in the cavity region of the R-MSA element and using the coordinate system shown in Fig. 2 (a), two equivalent magnetic currents $\vec{J}_{m\bar{a}}$ and $\vec{J}_{m\bar{b}}$ can be expressed as follows [1], [2], [4], [5];

$$\vec{J}_{mu} = \sigma_a(u) J^{00}_{mu} \cos m\phi_0 \delta(r-u)\delta(z)\hat{i}_{\phi_0}, \qquad (1)$$

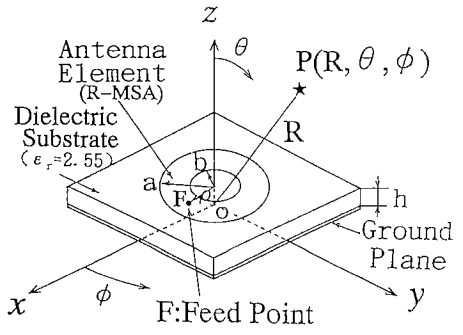

Fig. 1 Basic configuration of ring-shaped microstrip antenna (R-MSA).

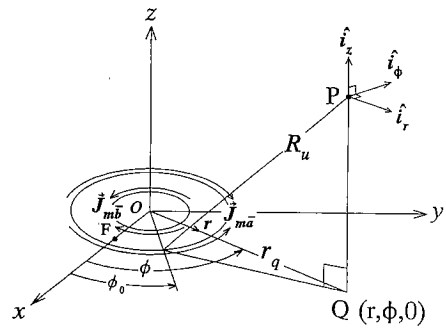

$\hat{i}_r, \hat{i}_\phi, \hat{i}_z$: Unit vector in cylindrical coordinate system.

(a)

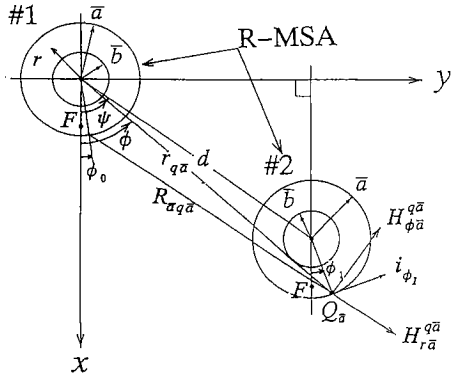

(b)

Fig. 2 Coordinate system for R-MSA array. (a) Isolated R-MSA element, (b) Two-element R-MSA array.

where

$$J^{00}_{mu} = E_0\left\{J_m(k_{mn}u) - \frac{J'_m(X_{mn})}{Y'_m(X_{mn})}Y_m(k_{mn}u)\right\}, \tag{2}$$

$$u = \bar{a}, \bar{b}$$

$$\sigma_a(i) = \begin{cases} +1, & \text{for } i = \bar{a}, \\ -1, & \text{for } i = \bar{b}, \end{cases} \tag{3}$$

and magnetic currents $\vec{J}_{m\bar{a}}$ and $\vec{J}_{m\bar{b}}$ are assumed to exist only on the xy-plane to simplify the following estimations. Moreover, J^{00}_{mu} denotes the maximum value of equivalent magnetic currents and E_0 denotes the maximum amplitude in the z-component of electric field at the outer ring edge of R-MSA element. Furthermore, $\bar{a}$ and $\bar{b}$ shown in Eq. (3) are the effective outer and inner ring radii that contain a fringing fields effect [8], and $\delta(z)$ is the delta function, $\hat{i}_{\phi_0}$ is the circumference unit vector of ϕ_0-direction in the polar coordinate system, $J_m(x)$ and $Y_m(x)$ denote Bessel's and Neuman's functions, respectively, and the primes are the derivatives with respect to x, X_{mn} is the eigenvalue of the TM_{mn0} mode excited in the cavity region, and k_{mn} is the wavenumber.

Vector potential $\vec{A}_{mu}$ is utilized to obtain the magnetic field that is generated by equivalent magnetic currents $\vec{J}_{mu}$, and mathematically can be expressed by following [5], [8], [9], as

$$\begin{aligned}\vec{A}_{mu} = \frac{\sigma_a(u)\varepsilon_0}{2\pi}\int_0^{2\pi}\{&J^0_{mu}\cos m\phi_0\cos(\phi_0-\phi)\hat{i}_\phi \\ &- J^0_{mu}\cos m\phi_0\sin(\phi_0-\phi)\hat{i}_r\} \\ &\times\frac{e^{-jk_0R_u}}{R_u}ud\phi_0\end{aligned} \tag{4}$$

where,

$$R_u = \sqrt{r_q^2 + u^2 - 2r_q u\cos(\phi_0-\phi) + z^2} \tag{5}$$

J^0_{mu} is the equivalent magnetic currents for which the mutual coupling between $J_{m\bar{a}}$ and $J_{m\bar{b}}$ of the isolated R-MSA element is taken into account. J^0_{mu} is corresponding to $J^0_{m\bar{a}}$ and $J^0_{m\bar{b}}$, namely $J^0_{m\bar{a}}$ contains the effect of mutual coupling of inner magnetic current $J_{m\bar{b}}$, and $J^0_{m\bar{b}}$ contains the effect of mutual coupling of outer magnetic current $J_{m\bar{a}}$, R_u denotes the distance between the edge magnetic currents and the observation point P, $\hat{i}_\phi$ and $\hat{i}_r$ are the circumference and radial unit vector in cylindrical coordinate system, ε_0 is the permittivity in free space and $\sigma_a(u)$ is given as Eq. (3) with $u = \bar{a}, \bar{b}$. Furthermore, the magnetic field at observation point P (R,Θ,ϕ) can be calculated using the following well-known relation:

$$\vec{H}_u = \frac{\nabla\nabla\cdot\vec{A}_{mu}}{j\omega\varepsilon_0\mu_0} - j\omega\vec{A}_{mu} \tag{6}$$

It is illustrated in Fig. 2 (b) that the element spacing is d and the arrangement angle of the two elements is ψ. Next, considering the coordinate system shown in Fig. 2 (b) and using Eq. (6), magnetic field $\vec{H}^{q_v}_u$ at point Q_v can be derived analytically by the method given in [5]. It corresponds to the magnetic field at the periphery of the outer or inner ring region in the #2 R-MSA element. This magnetic field $\vec{H}^{q_v}_u$ can then be decomposed into $H^{q_v}_{ru}$ and $H^{q_v}_{\phi u}$ components as follows:

$$\begin{aligned}H^{q_v}_{ru} = &-\sigma_a(u)\cdot j\frac{1}{2\pi\omega\mu_0} \\ &\times\int_0^{2\pi} mJ^0_{mu}\sin m\phi_0\left(jk_0+\frac{1}{R_{uq_v}}\right) \\ &\times\left\{r_{q_v}-\frac{u}{r_{q_v}}m_{2v}(d,\phi_0,\phi_1,\psi)\right\}\frac{e^{-jk_0R_{uq_v}}}{R^2_{uq_v}}d\phi_0 \\ &+ j\frac{\omega\varepsilon}{2\pi}\int_0^{2\pi} uJ^0_{mu}\cos m\phi_0\frac{m_{1v}(d,\phi_0,\phi_1,\psi)}{r_{q_v}} \\ &\cdot\frac{e^{-jk_0R_{uq_v}}}{R_{uq_v}}d\phi_0\end{aligned} \tag{7}$$

$$H_{\phi u}^{q_v} = \sigma_a(u) \cdot j\frac{1}{2\pi\omega\mu_0} \times \int_0^{2\pi} umJ_{mu}^0 \sin m\phi_0 \left(jk_0 + \frac{1}{R_{uq_v}}\right) \times \frac{m_{1v}(d,\phi_0,\phi_1,\psi)}{r_{q_v}} \cdot \frac{e^{-jk_0R_{uq_v}}}{R_{uq_v}^2} d\phi_0 - j\frac{\omega\varepsilon}{2\pi} \int_0^{2\pi} uJ_{mu}^0 \cos m\phi_0 \frac{m_{2v}(d,\phi_0,\phi_1,\psi)}{r_{q_v}} \cdot \frac{e^{-jk_0R_{uq_v}}}{R_{uq_v}} d\phi_0 \quad (8)$$

where

$$r_{q_v} = \sqrt{d^2 + v^2 + 2dv\cos(\psi - \phi_1)} \quad (9)$$

$$R_{uq_v} = \sqrt{r_{q_v}^2 + u^2 - 2r_{q_v}u\cos(\phi_0 - \phi)} \quad (10)$$

$$\sin(\phi_0 - \phi) = \frac{d\sin(\phi_0 - \psi) + v\sin(\phi_0 - \phi_1)}{r_{q_v}} \quad (11)$$

$$\cos(\phi_0 - \phi) = \frac{d\cos(\phi_0 - \psi) + v\cos(\phi_0 - \phi_1)}{r_{q_v}} \quad (12)$$

$$m_{1v}(d,\phi_0,\phi_1,\psi) = d\sin(\phi_0 - \psi) + v\sin(\phi_0 - \phi_1) \quad (13)$$

$$m_{2v}(d,\phi_0,\phi_1,\psi) = d\cos(\phi_0 - \psi) + v\cos(\phi_0 - \phi_1) \quad (14)$$

$u = \bar{a}, \bar{b}(\#1R - MSA)$ and $v = \bar{a}, \bar{b}(\#2R - MSA)$,

where μ_0 and k_0 are the permeability and the wavenumber in free space, and ω is the angular frequency. Furthermore, ϕ_0, ϕ_1 and ϕ are corresponds to the angular components shown in Fig. 2 (b).

Next, mutual admittance Y_{21} of this R-MSA array can be calculated using the EMF method which is described in Refs. [5] and [9]. The expression of Y_{21} can be written as

$$Y_{21} = \frac{Y_{\bar{a}\bar{a}21}J_{m\bar{a}}^0 + Y_{\bar{b}\bar{a}21}J_{m\bar{b}}^0}{J_m^{\#1}} + \frac{Y_{\bar{b}\bar{b}21}J_{m\bar{b}}^0 + Y_{\bar{a}\bar{b}21}J_{m\bar{a}}^0}{J_m^{\#1}} \quad (15)$$

where, $J_m^{\#1}$ is the equivalent magnetic current of the #1 R-MSA considered the effect of magnetic currents at the inner and outer ring edges, and

$$Y_{uv21} = \frac{P_{uv}}{J_{mu}^0 \times J_{mv}^{0*}} \quad (16)$$

where

$$P_{uv} = -\sigma_a(v) \cdot \int_0^{2\pi} \left(H_{ru}^{q_v}\frac{d\sin(\psi - \phi_1)}{r_{q_v}} + H_{\phi u}^{q_v}\frac{d\cos(\psi - \phi_1) + v}{r_{q_v}} \right) \times J_{mv}^{0*}\cos m\phi_1 v d\phi_1 \quad (17)$$

with J_{mv}^{0*} is the complex conjugate of J_{mv}^0. Substituting Eqs. (7) and (8) into Eq. (17), and then carrying out numerical integration of Eq. (17), the values of mutual admittance $Y_{21}(= Y_{12})$ can be obtained. Finally, mutual coupling $|S_{21}|$ can be expressed in terms of mutual admittance as follows:

$$|S_{21}| = |S_{12}| = \left|\frac{-2\hat{Y}_{12}}{(1 + \hat{Y}_{11})^2 - \hat{Y}_{12}^2}\right| \quad (18)$$

where $\hat{Y}_{11}$ and $\hat{Y}_{12}$ are the self and mutual admittances normalized by self conductance (G_{11}) of the isolated R-MSA, respectively.

2.2 Active Reflection Coefficient $|\Gamma|$ of R-MSA Array

In this section, active reflection coefficient $|\Gamma|$ corresponding to active impedance $Z_{in}^n(\theta_s, \phi_s)$, which may have usefullness in the designing of a phased array antenna, is investigated. In general, the active reflection coefficient $|\Gamma|(= |\Gamma(\theta_s, \phi_s)|)$ can be expressed as follows [6], [7]:

$$|\Gamma(\theta_s, \phi_s)| = \left|\frac{Z_{in}^n(\theta_s, \phi_s) - Z_{in}^n(0,0)}{Z_{in}^n(\theta_s, \phi_s) + Z_{in}^{n*}(0,0)}\right| \quad (19)$$

where, $Z_{in}^n(\theta_s, \phi_s)$ is the active input impedance at the nth element in the planar array with scan angle θ_s, ϕ_s. $Z_{in}^{n*}(0,0)$ is complex conjugate of $Z_{in}^n(0,0)$. Both impedances $Z_{in}^n(\theta_s, \phi_s)$ and $Z_{in}^n(0,0)$ of the array are determined by using the values of mutual impedance Z_{21} or mutual admittance Y_{21}. In this study, in order to compute the mutual admittance Y_{21} of the array we use the EMF method instead of the moment method given in Refs. [6] and [7]. Comparison of the data between this method [5], [9], [10] and the moment method is shown in Fig. A· 1 of Appendix, where both computed results were obtained using a 7×7 element square arrangement of planar array composed of rectangular MSA elements. As shown in the figure, both methods are agreed well within a desirable range for designing.

3. Consideration on Numerical and Experimental Results

In this section, the numerical data of mutual coupling $|S_{21}|$ for the dominant mode (TM_{110}) are compared with some experimental data. Subsequently, we describe the experimental data of circularly polarized (CP) R-MSA planar array as well as the computational data of active reflection coefficient $|\Gamma|$.

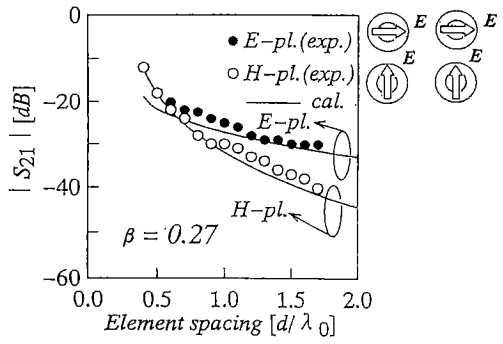

Fig. 3 Mutual coupling of two-element R-MSA array as a function of element spacing d/λ_0 ($h = 0.02\,\lambda_0$).

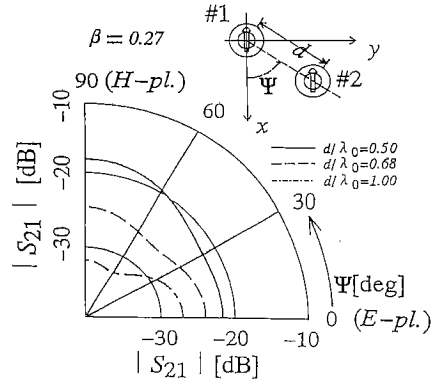

Fig. 4 Mutual coupling of two-element R-MSA array as a function of arrangement angle ψ for various element spacing ($h = 0.02\,\lambda_0$).

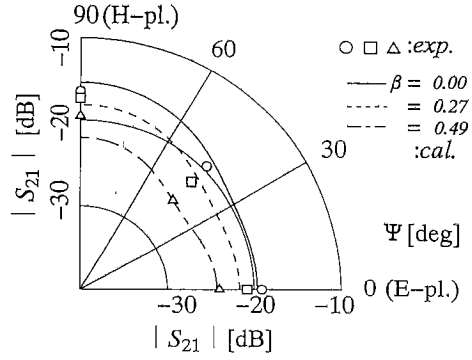

Fig. 5 Mutual coupling of two-element R-MSA array as a function of arrangement angle ψ for various ring ratio ($h = 0.02\,\lambda_0$, $d/\lambda_0 = 0.5$).

3.1 Mutual Coupling Effect in Two-Element R-MSA Array

First, mutual coupling $|S_{21}|$ in 2-element array is calculated using Eq. (18) as a function of element spacing d/λ_0 in both E- and H-plane arrangements. The computed results for the dominant mode (TM_{110}), then, are compared with the experimental data obtained from the array which is composed of R-MSA elements with ring ratio $\beta = 0.27$. The ring ratio β is set at 0.27 considering the condition of the impedance matching, size reduction and bandwidth. It is shown that satisfactory agreement was confirmed between the experimental data and the calculated ones as plotted in Fig. 3.

Next, mutual coupling $|S_{21}|$ as a function of arrangement angle ψ, is calculated for various element spacing d as illustrated in Fig. 4. It is of particular interest that for $d/\lambda_0 = 0.68$ and its vicinity, where λ_0 is free space wavelength, the values of mutual coupling $|S_{21}|$ are in uniformity at all arrangement angle ψ. The mutual coupling value of less than -23 dB can be achieved with element spacing of $d/\lambda_0 = 0.68$. The uniformity of mutual coupling is important to design circularly polarized (CP) array antenna, because the mutual coupling values in E- and H-planes should be the same in order to achieve a good axial ratio.

The mutual coupling as a function of arrangement angle ψ is also computed for various ring ratio β, for examples; some experiments are also carried out for a radiating element having a ring ratio of $\beta = 0$ (usual circular MSA), $\beta = 0.27$ or $\beta = 0.49$. In these experiments, element spacing of the test antennas were set at $d/\lambda_0 = 0.5$. Excellent agreement between computational and experimental data can be achieved for $\beta = 0.27$ as shown in Fig. 5.

The test sample of R-MSA array used in this experiments was fabricated on Teflon glass-fiber dielectric substrate, where $\varepsilon_r = 2.55$, $\sigma = 5.8 \times 10^7$ S/m and $\tan\delta = 0.0018$, and thickness $h = 0.020\,\lambda_0$. The calculated values of $|S_{21}|$ agreed well with the experimental results, although the effect of the dielectric substrate (Teflon glass-fiber) was not taken into account.

3.2 Radiation Properties of R-MSA Planar Array

It is well known that application to many communication systems require a circularly polarized (CP) planar array [5]. For this reason, a CP R-MSA planar array is designed here using the previous results of $|S_{21}|$. Figure 6 (a) shows the basic configuration of a typical CP R-MSA element. The perturbation segment ($\Delta S/2$) is set at the periphery of R-MSA element to excite the circular polarization [5]. The basic configuration of a 4×4 element CP R-MSA planar array is illustrated in Fig. 6 (b).

The element spacing $d = 0.68\,\lambda_0$ is selected for the array, taking the previously discussed mutual coupling effect into consideration. Moreover, the input impedance (Z_{in}) of each R-MSA element is matched to that of main feedline M of the subarray unit using $\lambda/4$ impedance transformers T_{f1}, T_{f2} and T_{f3}, where λ is the wavelength in the feedline. After designing the 4×4 element planar array, the radiation properties were measured at the C-band.

Figure 7 shows the return loss characteristic of this array. As shown in the figure, -12 dB return loss and about 3 % bandwidth of $VSWR = 2$ can be achieved in

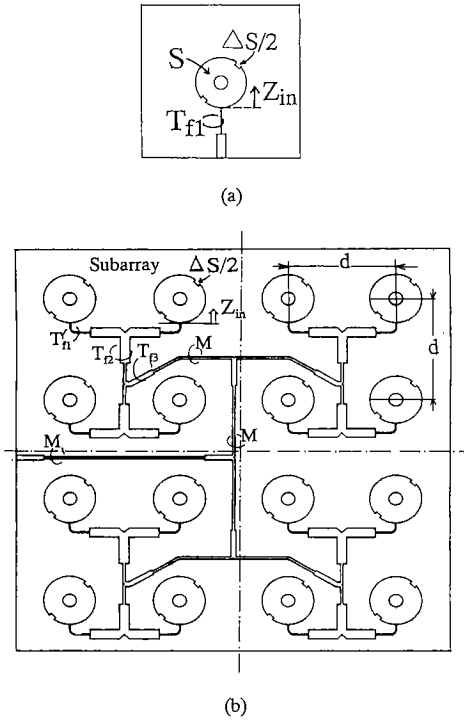

Fig. 6 Basic arrangement of planar array antenna and its element ($d = 0.68\,\lambda_0$, $\beta = 0.27$). (a) Configuration of CP R-MSA element, (b) Basic configuration of 4×4 element CP R-MSA array.

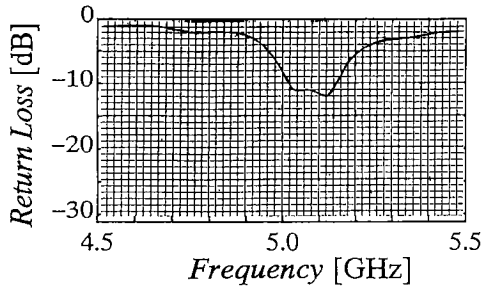

Fig. 7 Return loss property of CP R-MSA array ($f_0 = 5.08\,[GHz]$, $h = 0.02\,\lambda_0$, $d = 0.68\,\lambda_0$, $\beta = 0.27$, $\Delta S/S = 0.0176$).

this antenna. Furthermore, the radiation pattern of this CP R-MSA array was measured and plotted in Fig. 8. As shown in the figure, an axial ratio of less than 0.5 dB can be accomplished over the main beam region of the radiation pattern for this array. In addition, the axial ratio as well as the antenna gain as a function of frequency are plotted in Fig. 9. It is also shown here that a typical gain is about 18 dBi in this array.

3.3 Active Reflection Coefficient $|\Gamma|$ of R-MSA Array

In order to estimate active reflection coefficient $|\Gamma|$ of this type of phased array, two typical arrangements, equilateral and square arrangements, are adopted in this investigation, as shown in Fig. 10. As shown in Fig. 11 and Fig. 12, θ_s is the scan angle, and ϕ is the angle to the x-axis, where the xz-plane ($\phi = 0$) corresponds to E-

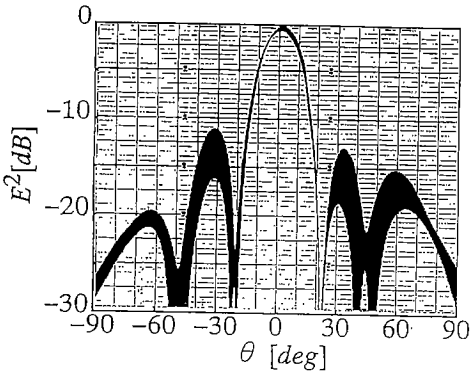

Fig. 8 Radiation pattern of 4×4 element CP R-MSA array ($f_0 = 5.08\,[GHz]$, $h = 0.02\,\lambda_0$, $d = 0.68\,\lambda_0$, $\beta = 0.27$, $\Delta S/S = 0.0176$).

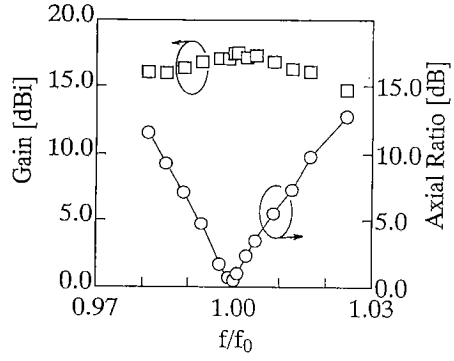

Fig. 9 Gain and axial ratio characteristics of CP R-MSA as a function of frequency.

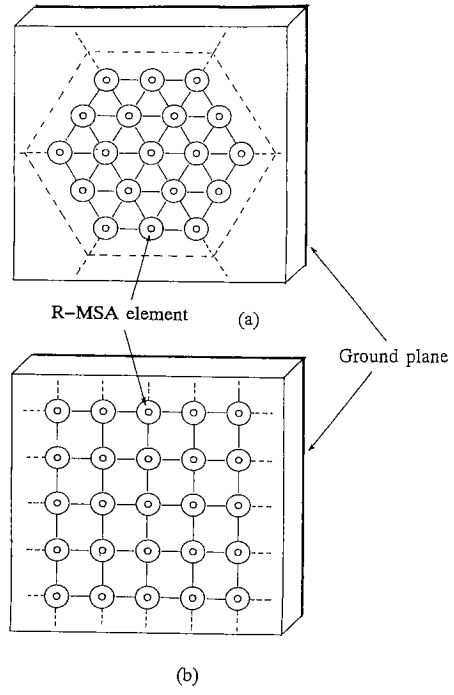

Fig. 10 Basic configuration of planar array antenna. (a) Equilateral arrangement, (b) Square arrangement.

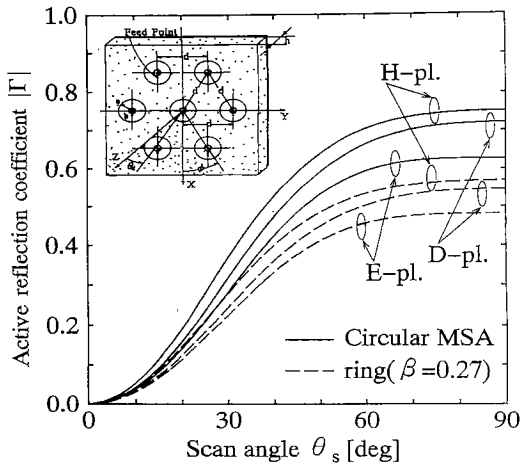

Fig. 11 Active reflection coefficient $|\Gamma|$ for equilateral configuration as a function of scan angle θ_s (7 element, $d/\lambda_0 = 1/\sqrt{3}$, $h/\lambda_0 = 0.04$).

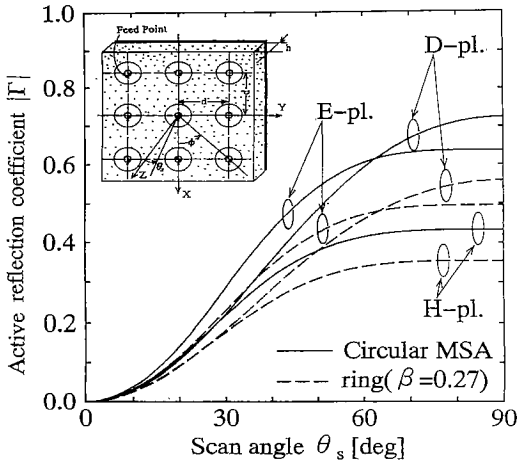

Fig. 12 Active reflection coefficient $|\Gamma|$ for square configuration as a function of scan angle θ_s (3×3 element, $d/\lambda_0 = 0.5$, $h/\lambda_0 = 0.04$).

plane scanning and the yz-plane ($\phi = \pi/2$) corresponds to H-plane scanning.

It is well known that the subarrays shown in Fig. 10 can be expanded into a larger scale array by introducing symmetrical arrangement. In order to obtain some useful designing data, two types of radiating element, circular MSA ($\beta = 0$) and R-MSA ($\beta = 0.27$), are considered as elements for both equilateral and square arrangements. For equilateral configurations, a 7-element array with element spacing $d/\lambda_0 = 1/\sqrt{3}$ is employed. Active reflection coefficient $|\Gamma|$ is then calculated using Eq. (19) for the center element, and the result is plotted in Fig. 11.

In a similar way to the equilateral one, a square configuration is also considered using a 3×3 element array with element spacing $d/\lambda_0 = 0.5$. The computational result of active reflection coefficient is then plotted in Fig. 12 for the center element. An interesting result is shown here; a lower reflection coefficient is achieved for the R-MSA element compared with a usual circular MSA array for E, H and D-planes.

4. Conclusions

In this paper the mutual coupling $|S_{21}|$ in a 2 element R-MSA array was investigated analytically as well as experimentally. The EMF method based on the cavity model was used in the analytical study. It is shown that the computed values of the mutual coupling in the 2-element array agreed well with the experimental results in both E- and H-planes. Using the aforementioned results, a CP-wave planar array was fabricated using R-MSA elements. The results confirmed excellent properties of this planar array in both radiation pattern and axial ratio characteristics. Furthermore, the active reflection coefficient $|\Gamma|$ of this type of array was also studied analytically. The results showed that lower active reflection coefficient $|\Gamma|$ was achieved for the array composed of R-MSA elements in both equilateral and square arrangements. The results of the experiments also demonstrated that the R-MSA investigated here can be considered to be applicable as an antenna element of the planar array antenna system.

References

[1] El-Khamy, S.E., El-Awadi, R.M. and El-Sharrawy, E.-B. A., "Simple analysis and design of annular ring microstrip antennas," *IEE Proc.*, vol.133, pt. H, no.3, pp.198–202, Jun. 1986.

[2] Bahl, I.J., Stuchly, S.S. and Stuchly, M.A., "A new microstrip radiator for medical applications," *IEEE Trans. Microwave Theory Tech.*, vol.MTT-28, no.12, pp.1464–1468, Dec. 1980.

[3] Tsutsumi, T., Tsuda, S., Matsui, A. and Haneishi, M., "Radiation properties of circularly polarized microstrip ring antenna excited by dominant mode," *Proc. ISAP '92*, Sapporo, Japan, pp.805–808, Sep. 1992.

[4] Das, A., Das, S.K. and Mathur, S.P., "Radiation characteristics of higher-order modes in microstrip ring antenna," *IEE Proc.*, vol.131, pt. H, no.2, pp.102–106, Apr. 1984.

[5] Haneishi, M. and Suzuki, Y., "Circular polarization and bandwidth," Chapt. 4 in *Handbook of Microstrip Antennas*, edited by James, J.R. and Hall, P.S., Peter Peregrinus Ltd., 1989.

[6] Pozar, D.M., "Analysis of finite phased arrays of printed dipoles," *IEEE Trans. Antennas and Propag.*, vol.AP-33, no.10, pp.1045–1053, Oct. 1985.

[7] Pozar, D.M., "Finite phased arrays of rectangular microstrip patch," *IEEE Trans. Antennas and Propag.*, vol.AP-34, no.5, pp.658–665, May 1986.

[8] James, J.R., Hall, P.S. and Wood, C., *Microstrip Antennas – Theory and Design*, Peter Peregrinus Ltd., 1981.

[9] Haneishi, M., Yoshida, Y. and Tabeta, M., "A design of back-feed type circularly polarized microstrip disk antennas having symmetrical perturbation element by one-point feed," *Trans. IEICE*, vol.J64-B, no.7, pp.612–618, Jul. 1981.

[10] Abe, T., Haneishi, M. and Kuroda, S., "A consideration on scan performance of rectangular microstrip antenna array," *1991 Spring Natl. Conv. Rec., IEICE*, B-104.

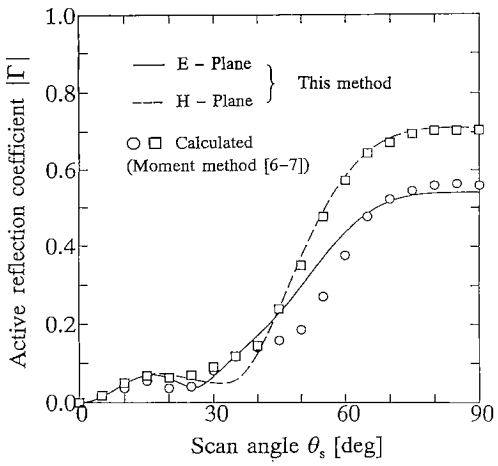

Fig. A· 1 Comparison of computational results in active reflection coefficient $|\Gamma|$ using this method and the moment method in Refs. [6], [7] (7×7 element square arrangement array composed of rectangular microstrip antenna elements, and antennas size is $0.3\,\lambda_0 \times 0.3\,\lambda_0$, $d/\lambda_0 = 0.5$, $h/\lambda_0 = 0.04$).

Appendix

In this paper, the EMF method based upon the cavity model is proposed to compute active reflection coefficient $|\Gamma|$ shown in Sect. 2. To check the validity of the proposed method a comparison with the moment method [6], [7] is taken as plotted in Fig. A· 1. The comparison of the two methods is given for the same sample of array with a 7×7 element planar MSA array composed of rectangular MSA elements with patch size $0.3\,\lambda_0 \times 0.3\,\lambda_0$, and another parameters are $\varepsilon_r = 2.55$, $d/\lambda_0 = 0.5$ and $h/\lambda_0 = 0.04$. It is demonstrated that the method applied here is in satisfactory agreement with the moment method, as shown in Fig. A· 1.

Motohiko Kobayashi was born in Tokyo, Japan, on January 18, 1970. He received the B.E. and M.E. degrees in electrical engineering from the Saitama University in 1993 and 1995, respectively. Since April 1995 he has joined the Tokyo Electric Power Company Corporation, Tokyo, Japan. His research interest was analysis of microstrip antenna.

Eko Tjipto Rahardjo was born in Pati, Indonesia, on April 22, 1958. He received the Insinyur (Ir.) degree from the University of Indonesia, Jakarta, Indonesia, and M.S. degree from the University of Hawaii, Honolulu, U.S.A., all in electrical engineering, in 1981 and 1987, respectively. He joined to the Department of Electrical Engineering, the University of Indonesia as an assistant lecturer in 1982 and presently he is a senior lecturer. He is now on leave from the University of Indonesia pursuing the Ph.D. program in the Saitama University, Urawa, Japan, under the Hitachi Scholarship Foundation. His current main research is in the microstrip antenna.

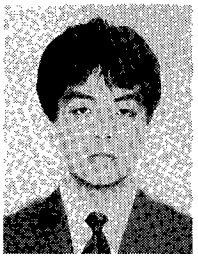

Shin-ichiro Tsuda received the B.E. and M.E. degrees in electrical engineering from the Saitama University in 1991 and 1993, respectively. Since April 1993 he has joined the Sony Corporation, Tokyo, Japan, and since December 1994 he has been promoted to a new position in the Personal Telecom Division, Sony Electronic Inc., U.S.A.

Misao Haneishi received the B.S. degree in electrical engineering from the Saitama University in 1967, the M.S. degree in electrical engineering from the Tokyo Metropolitan University in 1969 and the Dr. Eng. degree from the Tokyo Institute of Technology in 1981. In 1969, he joined the Faculty of Engineering in the Saitama University and since then he has enganged in the research of microwave antennas engineering. He is now the professor of electrical engineering at the Saitama University.